Utilizing Hyperspectral Remote Sensing for Gradation of Soils

Jordan Ewing[1], Thomas Oommen[2], Paramsothy Jayakumar, and Russel Alger[4]

1. Doctoral Student, Michigan Technological University, Houghton, Michigan, email: jjewing@mtu.edu
2. Associate Professor, Department of Geological Engineering, Michigan Technological University, Houghton, Michigan, email: toommen@mtu.edu
3. US Army CCDC Ground Vehicle Systems Center, Warren, Michigan, email: paramsothy.jayakumar.civ@mail.mil
4. Director of the Institute of Snow Research, Keweenaw Research Center, Houghton, Michigan, email: rgalger@mtu.edu

Abstract:

Remote sensing is the process of measuring the property of an object from a distance without having direct contact with the object of interest. Remote sensors collect electromagnetic energy reflected or radiated from the object. When the remote sensors have the sensitivity to detect narrow bandwidths (5-10 nm) of the electromagnetic spectrum, they are referred to as hyperspectral remote sensing. Hyperspectral remote sensing provides us the opportunity to look at the unique signatures and characteristics of materials. In this research, we are particularly interested in the application of hyperspectral remote sensing to characterize soil gradation. The specific objective of this work is to explore the application of hyperspectral remote sensing to be used as an alternative to traditional soil gradation estimation. The advantage of such an approach is that it would provide the soil gradation without having to obtain a field sample. This information can be vital to identify the soil type, soil strength, permeability/hydraulic conductivity, and other properties that are correlated to the gradation of the soil. Our study demonstrates a correlation between hyperspectral data, the percent gravel and sand composition of soil. Using this correlation one can predict the percent gravel and sand within a soil; and in turn calculate the remaining percent of fine particles. Thus, giving the entire gradation breakdown of a soil. This breakdown then allows one to classify it within the Unified Soil Classification System (USCS).

Introduction:

The Unified Soil Classification System (USCS) is the standard for classifying soil based on their gradation (ASTM D-2487). The USCS is used for helping to keep soil classification organized across the board. The gradation is an important characteristic that has an influence on the physical and mechanical properties of the soil. Studies show that the gradation of soils carry important details of the soil's mechanical properties and that one can create an index to find correlations to these values. (Cola 2002). Kuenza (2004) has looked into gravel and sand composition of soils in mountainous areas with slope instability; based on the amount of sand versus the amount of gravel present will tell you which particle size has a more dominating influence over the soil's stress-strain behavior for an undrained torsional shear test. Presently, soil gradation is primarily done via sieve analysis (also called a gradation test).

The percentage of gravel and sand content in a soil influences the shear strength and dilatancy of sand-gravel mixtures. Therefore, knowing the gradation of the soil can be helpful to better estimate the soil's properties (Simoni 2004). While gradation is a very useful metric for geotechnical engineering, its estimation requires in-situ sample collection. The traditional approach of in-situ sample collection and sieve analysis can be laborious, costly, and difficult to attain in inaccessible or unfriendly territories. Therefore, ways to remotely characterize gradation can be of significant benefit for many applications.

One such application is in the mobility of military vehicles in unknown territories. There is present work being done where terrain strength characteristics and land mapping for autonomous mobility and simulation modeling are quintessential. The methods for the past models have relied heavily on in-situ measurement, which requires you to gather the soil from an area of interest, which can be hard to obtain or impossible in war-zones and inaccessible territories and are looking to be improved (Dasch & Jayakumar 2016). Therefore, we present an alternative method for predicting the gradation of the soil using remote sensing that would be particularly beneficial for inaccessible territories.

With the rapid increase of computational capabilities and sensor improvements, remote sensing has developed into a more time efficient and accurate tool; which will continue to grow with new and emerging ideas (Minasny 2016). Remote imagery provides a means of quick and efficient data collection for rapid assessment of an area. Work has been done on analyzing the use of different means via cameras, UAV, and satellite to provide a way to measure sand lower bound friction angles and bearing strength (Stark 2017). Hyperspectral imaging has already worked towards improving our ability to do anomaly detection, target recognition, and background characterization (Shaw 2003).

Studies using both multispectral and hyperspectral sensors show promise in the use of optical remote sensing to provide a new novel method for improving the mapping of soils (Sousa 2018). Using hyperspectral data one can predict different features/characteristics of bare soil, and certain wavelengths may provide a means of identifying/distinguishing certain features (Vohland 2017).

Hyperspectral remote sensing has the capability of determining attributes such as clay and sand content of a soil within laboratory and field. This could be especially useful when a large number of soil analysis needs done and may provide a real-time method for field data collection (Dematte 2010). Expanding beyond this, studies have already shown promise in developing a soil index, so as to help improve the classification of different colored sands based on both color and curvature of reflectance spectrums. Work still needs to be investigated for differing water conditions, grain size distribution, and other factors (Lucas 2002).

Currently, there is research being done on the best algorithms to implement for processing hyperspectral data to better classify different land cover types. Great success has already been found using support vector machine (SVM) methods for classifying hyperspectral data over multiple land cover types (Melgani 2004). Hyperspectral imaging of topsoil with the use of regression modeling has proved to be able to predict sand and clay percentages in a bare field (Selige 2006).
This method is a rapid and non-destructive means to measure the soil gradation as we propose to do similarly here. Where they utilize bands in the 2200-2400 nm range for predicting sand, we will use only the visible and near infrared (NIR) range (400-1000 nm). In our study, we verify the applicability of hyperspectral remote sensing to characterize the gradation of five different soil types.

Method

Soils

In this study, we analyzed five different soil types obtained from the Keweenaw Research Center (KRC) that are used for testing different terramechanics properties. These soils are labeled as Fine, Coarse, Rink, Stability, and 2NS which have varying amounts of sand, gravel, and fine particles. The specifics for these soils are listed in Table 1. The locations of these soils at KRC are shown in Figure 1.

Table 1: KRC Soil Information. D10 is grain diameter at 10% passing, D30 is grain diameter at 30% passing, and D60 is grain diameter at 60% passing. Cu is the coefficient of uniformity. Cc is the coefficient of curvature. USCS is the Unified Soil Classification for the Soil.

	Fine	Coarse	Rink	Stability	2NS
% Gravel	0.0	16.8073	10.7	31.1	0.6
% Sand	40.6	73.73772	66.4	58.8	97.3
% Fine	59.4	9.454973	23.0	10.0	2.1
D10	0.0151	0.085	0.015	0.075	0.175
D30	0.043	0.27	0.12	0.25	0.315
D60	0.076	0.38	0.25	2.65	0.7
Cu	5.03	4.5	16.7	35.3	4.0
Cc	1.61	2.3	3.8	0.3	0.7
USCS Classification	ML = Sandy Silt	Sp-SM = Poorly Graded Sand with Silt and Gravel	SM = Silty Sand	SW-SM = Well Graded Sand with Silt and Gravel	SP = Poorly Graded Sand

Figure 1: Five soil locations on-site at the Keweenaw Research Center, Houghton, Michigan.

Lab Tests

The study was conducted in the lab, with each of the five soils placed into their individual bin with dimensions roughly 2ft x 2ft x 1 ft (Length x Width x Height). These were then set in a row under a series of work lights, and a track to have the hyperspectral camera move over the soils in a straight and level manner as shown in Figure 2.


Figure 2: Shows the lab setup of the 5 KRC soils. The soils in order from bottom left to top right: 2NS, Stability, Rink, Coarse, and Fine. Above each bin are two 500-Watt work lights, and the middle bar is the track the hyperspectral camera is moved along.

Remote Sensing Background

Most everyday cameras operate within three bands, red, green, and blue. These cameras provide us the color images we see in regular photograph. However, there are many bands in the electromagnetic (EM) spectrum to which certain cameras are able to distinguish. If light was reflected from a smooth white surface, one would receive a 100% reflectance since nothing is absorbed into the material. Most objects have color, roughness, texture which all change the amount of light reflected back to the camera. The reflectance values for each different wavelength

is then recorded by the camera, which is then processed and analyzed to produce a multitude of information. Hyperspectral and multispectral cameras work by taking this reflected EM energy from the surface and read the response.

Hyperspectral and multispectral imaging are similar in the sense that they both collect different bands of light other than just the visible spectrum. Whatever platform the cameras may be mounted to, the final goal remains the same for both, which is to create a comprehensive image of the area with specific spectral reflectance values (Fisher 2006). Multispectral imaging has only a small number of bands going up to around 10 bands, with a wider wavelength range; while hyperspectral imaging may contain hundreds of bands that are spectrally narrow in wavelength. Figure 3 displays the bandwidth and the number of bands difference between the hyperspectral and multi-spectral imaging.

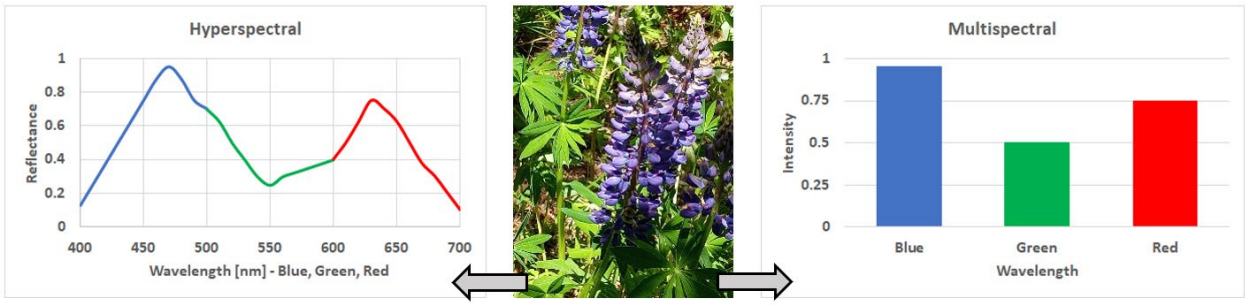

Figure 3: Shows the difference in both the number and width of bands for hyperspectral (Left) and multispectral (Right) imaging.

Just like with regular cameras the improvement of spatial-resolution allows to distinguish an image easier, as shown in figure 4. Similarly, a hyperspectral camera has a much better spectral resolution over a multispectral camera. The improvement in spectral resolution has shown to be powerful in identifying the unique characteristics of the material. Hence, a hyperspectral camera was chosen over a multispectral camera for this study to obtain the unique spectral behavior of the soils with respect to the change in gradation and other characteristics.

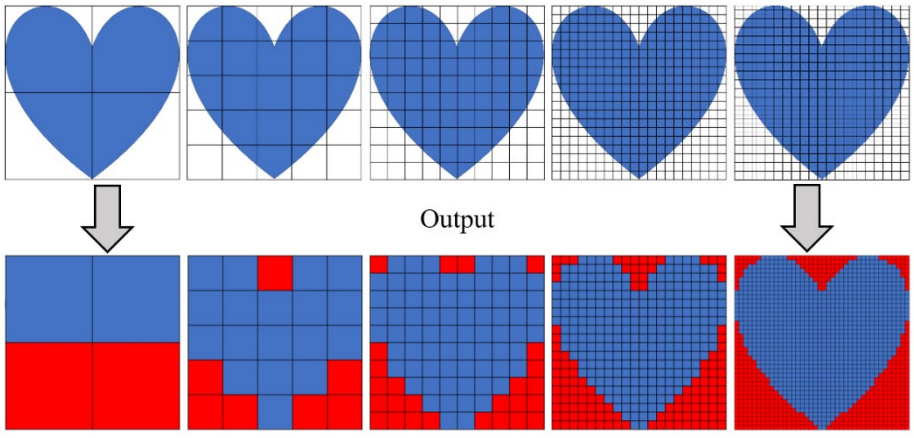

Figure 4: An illustration of spatial-resolution as it relates to pixel size. Lowest spatial-resolution (left) to highest spatial-resolution (Right). (2x2, 5x5, 10x10, 20x20, 40x40).

Sensors and Hardware

In this study, different spectral resolution hyperspectral cameras were used: a BaySpec OCI-F hyperspectral camera and a very high-resolution ASD spectral radiometer. This was done as a way of checking if more economically affordable hyperspectral cameras with a slightly lower spectral resolution could also be used to detect the similar features that the ASD spectral radiometer identified. This BaySpec camera (shown in figure 5) has a range of 400 – 1000 nm covering the entire visible (VIS) spectrum and some of the Near Infrared (NIR) region with roughly 5-7 nm full width at half max (FWHM) spectral resolution and 120 different bands. It is a push-broom camera, meaning it collects images as it moves in a straight line. The width of the scan line is known as the swath width. Taking images at rates of up to 60 frames per second (fps), it also has a spatial resolution of 800 pixels (swath width) by the scan-length. The camera is factory calibrated (calibration fixed permanently). It is equipped with a 16 mm (21° FOV) lens. The full technical aspects of this camera are listed in the BaySpec manual (BaySpec 2018).

Figure 5: Shows the BaySpec hyperspectral camera used for recording these values. The range of camera is from 400 – 1000 nm.

A high-resolution ASD spectral radiometer was also used; which has a useable band range from 400 to 2500 nm. The range from 350-399 nm has a lot of noise which makes the data unusable (Zwissler 2016). The device has a total of 512 bands in the visible-NIR range (350-1000nm), roughly 600 bands in the SWIR1 range (1000-1830nm), and similarly in the SWIR2 range (1830-2500 nm). The spectral resolution is: 3 nm (FWHM) at 700 nm, 10 nm (FWHM) at 1400 nm, and 10 nm (FWHM) at 2100 nm. Square spatial pixels are: 1.4 nm for 350 - 1000 nm and 2 nm for 1000 - 25000 nm. The fiber optic cable is run from the device into a pistol grip, and then a (1 degree) scope was attached to the grip. The device was facing at NADIR to the soil, during data collection, at the same location as the BaySpec camera at the center of each bin. The reflectance values of the region being scanned are collected in CSV format. Full technical aspects of the ASD spectral radiometer are listed in the ASD spectral radiometer manual (ASD Inc. 2010).

In order to collect the volumetric water content, a CR1000X is used with the CS615 probes. The CR1000X full technical aspects can be located in the Campbell Scientific Manual for the device (Campbell 2018; Campbell 1996). The CS615 water content probes are set to record the water content average over a 15-minute interval. The probes being 12 inches in length are placed into the soil at around an angle so as to be fully submerged into the soil and reach the bottom of the bin.

Laboratory Testing Methodology

First the volumetric water content probes were inserted into the bins and the water content was collected for 15 minutes. The average moisture content was then recorded for each of the soil bins. After the time allotted, the probes were removed and the work lights were turned on. The BaySpec camera was loaded onto a trolley which was then moved at NADIR across all five bins. Once images were collected, the BaySpec CubeCreator automatically combines all the individual slices and stitches them into one wide image. This then is used to highlight each individual bin and see the average reflectance curve over that area of interest. Each wavelength recorded will have its own specific/unique value. For example, red reflectance at 700 nm wavelength could be 20%, 0.2, while blue reflectance at 500 nm wavelength is 30%, 0.3. Figure 6 shows the soil bins (color image), the area captured by the camera (grey scale), and the hyperspectral plot after the software averages the pixel values for one of the trials done with the BaySpec camera. The BaySpec camera tested the soils at varying water contents ranging from 2 to 5% moisture content, with the Stability soil having one trial with 8%.

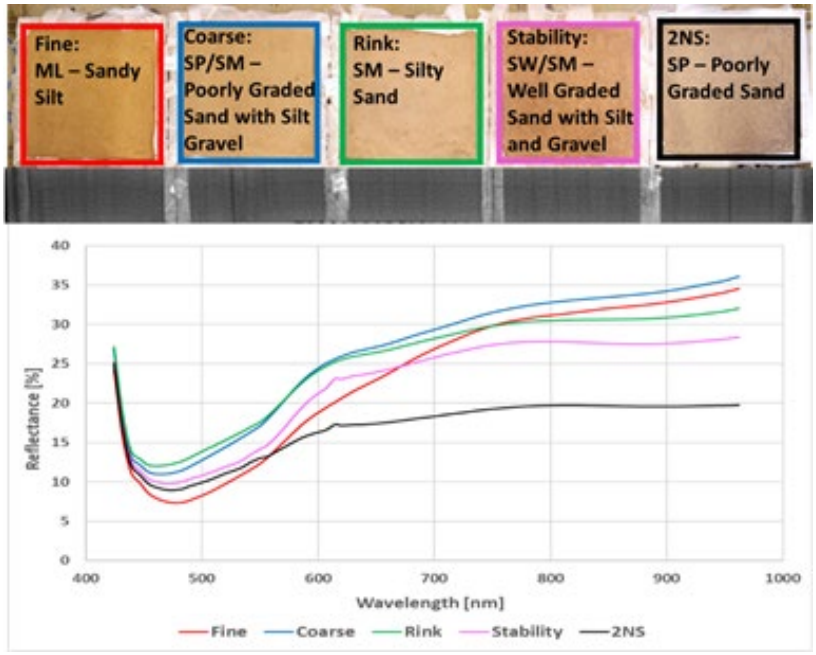

Figure 6: Shows the hyperspectral plots for each soil. Each colored box and corresponding line is a different soil type. Going from left to right: Fine, Coarse, Rink, Stability, and 2NS. The range of the camera is from 400 – 1000 nm.

The ASD spectral radiometer is then placed with the optical gun facing directly down at NADIR to the soil in the center. It was placed in such a manner that there were no shadows being cast onto the soil. A series of 10 consecutive tests were done over this area and then averaged to get the final reflectance for each soil type.

Once all the soils had been recorded on both devices, the lights were shut off and water was poured onto the soils via a watering can to simulate rainfall. The BaySpec camera was not used after the

first test due to processing time of the images collected, so it will only be examining drier conditions.
Different moisture content levels were tested ranging from 2 to <15% by adding various amounts of water in between trials and allowing around 10-15 minutes for the water to be absorbed by the soil. Then the process was repeated using only the ASD spectral radiometer to collect this data. The soil images and values from both sensors are then processed, and reflectance curves are gathered for each soil bin.

Results – Soil Classification Index

Based on these hyperspectral curves, a soil classification index was created to calculate a "Curve Index" for each soil, Equation 1. The developed index provides a means to identify the percent sand and gravel within a soil using hyperspectral remote sensing. Leaving the remaining amount of soil to be comprised of fine particles. Needing only the reflectance values at 550, 600, and 650 nm range of a hyperspectral image, the range is within the visible spectrum (Figure 7). These values we feel are representative of roughly the first 4-6 inches of the soil and did not vary much with water being added, increasing the moisture content of the soil. The index was checked at different moisture contents by adding water to the soil ranging from 0 to 4000 mL, see Figure 8.

Equation 1: Soil Classification Index = (R650 - R550) / R600

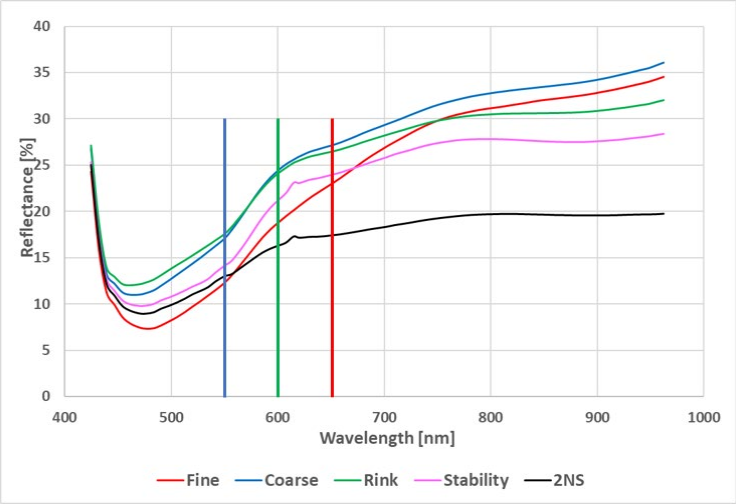

Figure 7: Shows the hyperspectral plots for each soil and the location of the needed values for the soil classification index.

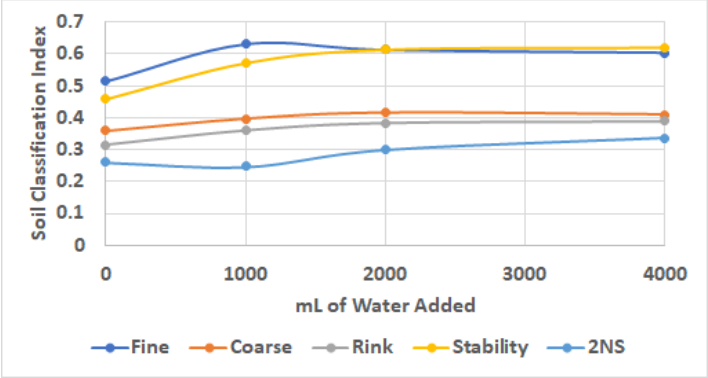

Figure 8: Shows the soil classification index against different amounts of water being added to the soil with a range of 0 to 4000 mL.

With the exception of Stability, due to a few outliers in the dry conditions, the soil classification index remained fairly stable. Once checked that the curve index remained fairly stable throughout varying moisture conditions, trends between the % gravel and % sand of the soils were examined. Figure 9 shows the relationship for both % gravel and % sand verses the soil classification index when the soil moisture content ranges from 2% to less than 15% moisture content, when using the ASD FieldSpec spectral radiometer. Results show that we only had difficulty with one type of soil for predicting the % gravel, but the trend did not fail even when the soil moisture was increased. The prediction for % sand, however, worked for all the five soil types, at varying moisture contents. Next, the relationships for when conditions are known about the moisture content: 2 to < 3%, 3 to < 5%, 5 to < 10%, and 10 to < 15% moisture content are shown in Figure 10 with % gravel in orange and % sand in blue.

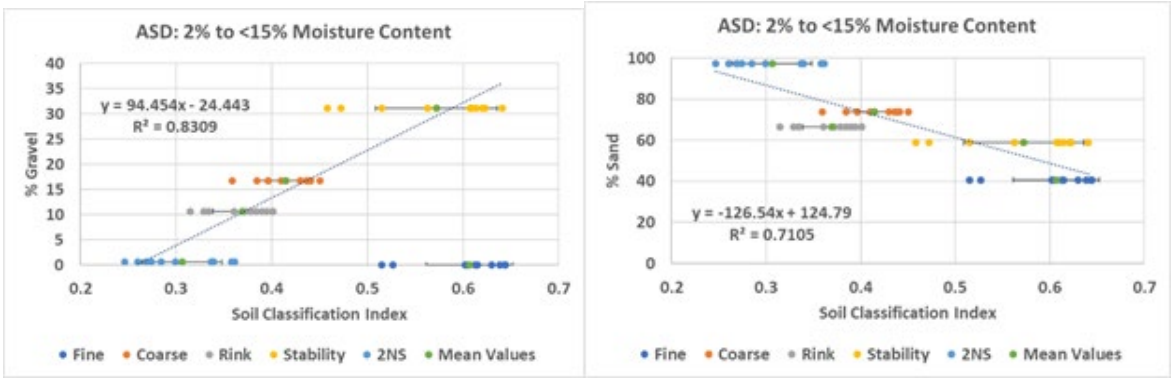

Figure 9: Trend lines for % sand and % gravel content among the five soils as recorded by the ASD FieldSpec spectral radiometer.

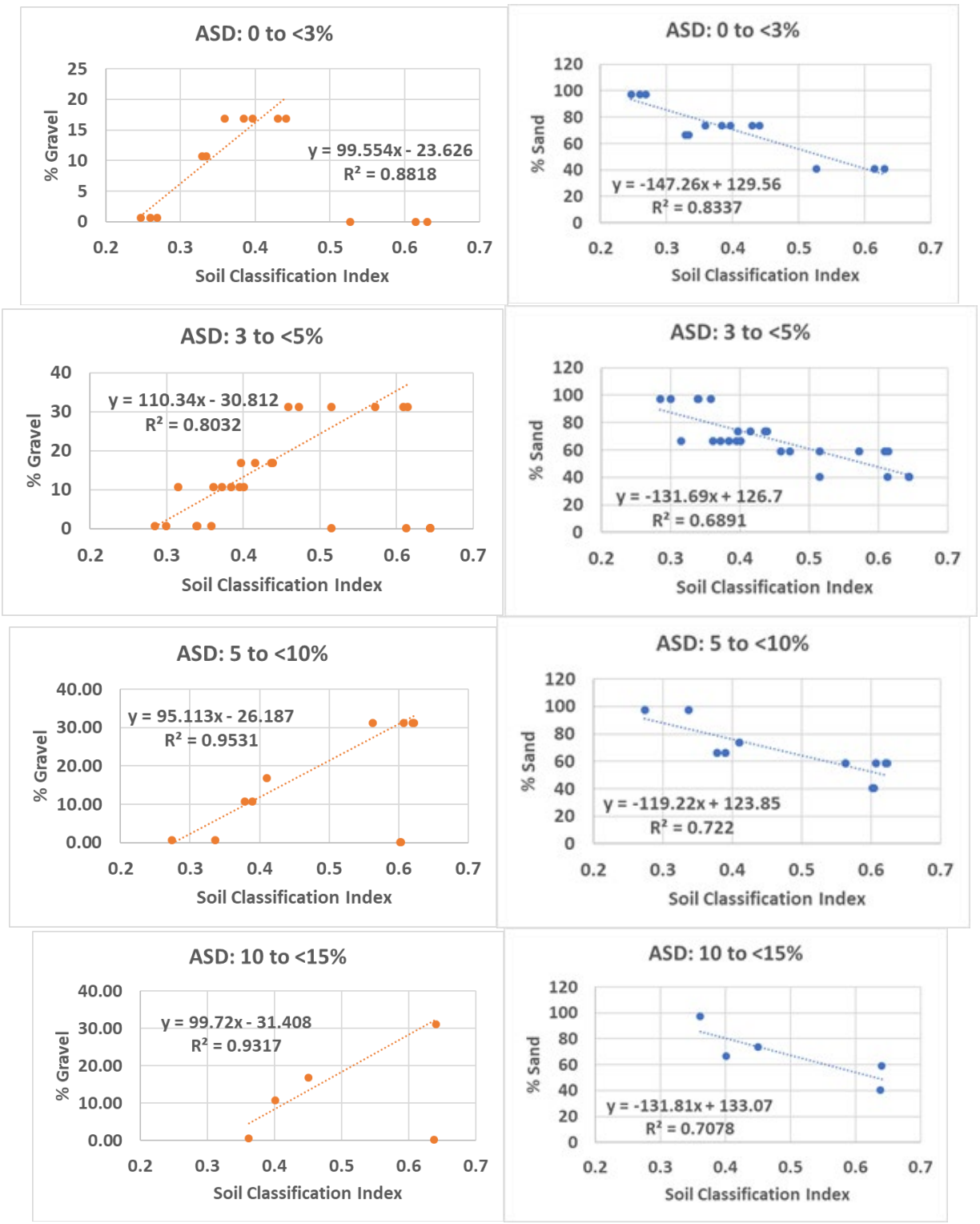

Figure 10: Each plot shows the soil classification index vs. % Gravel (Orange) or % Sand (Blue) where moisture content starts at around 2% (top) and increases to about 15% (bottom).

The BaySpec hyperspectral camera was also used to find similar trends. The BaySpec camera was tested for values ranging from 2-5% moisture content, with one soil (stability) having a single trial at 8%, and the plots are displayed in Figure 11.

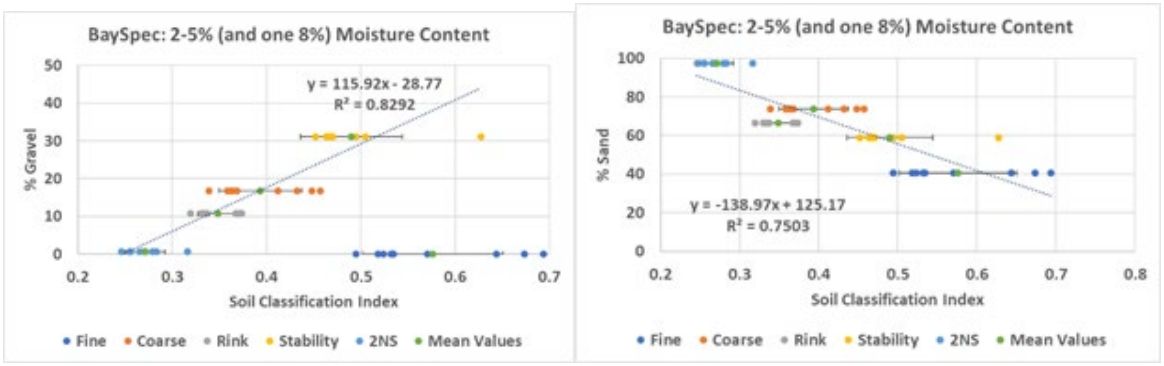

Figure 11: Trend lines for % sand and % gravel content among the five soils as recorded by the BaySpec hyperspectral camera.

When compared to the ASD the trendlines for both % gravel and % sand verses the soil classification index, have similar trends. The BaySpec and ASD trends slightly differ, while maintaining an accuracy of 86.2% (BaySpec) and 80% (ASD) for percent gravel estimation when under 5% moisture content. The % sand trends between the ASD and BaySpec devices are nearly parallel, while the prediction accuracy is either 73.3% (ASD) or 77.9% (BaySpec), also under 5% moisture content. Note that each trendline and its corresponding accuracy, was made in accordance to each device's collected set of data as seen in Figure 12.

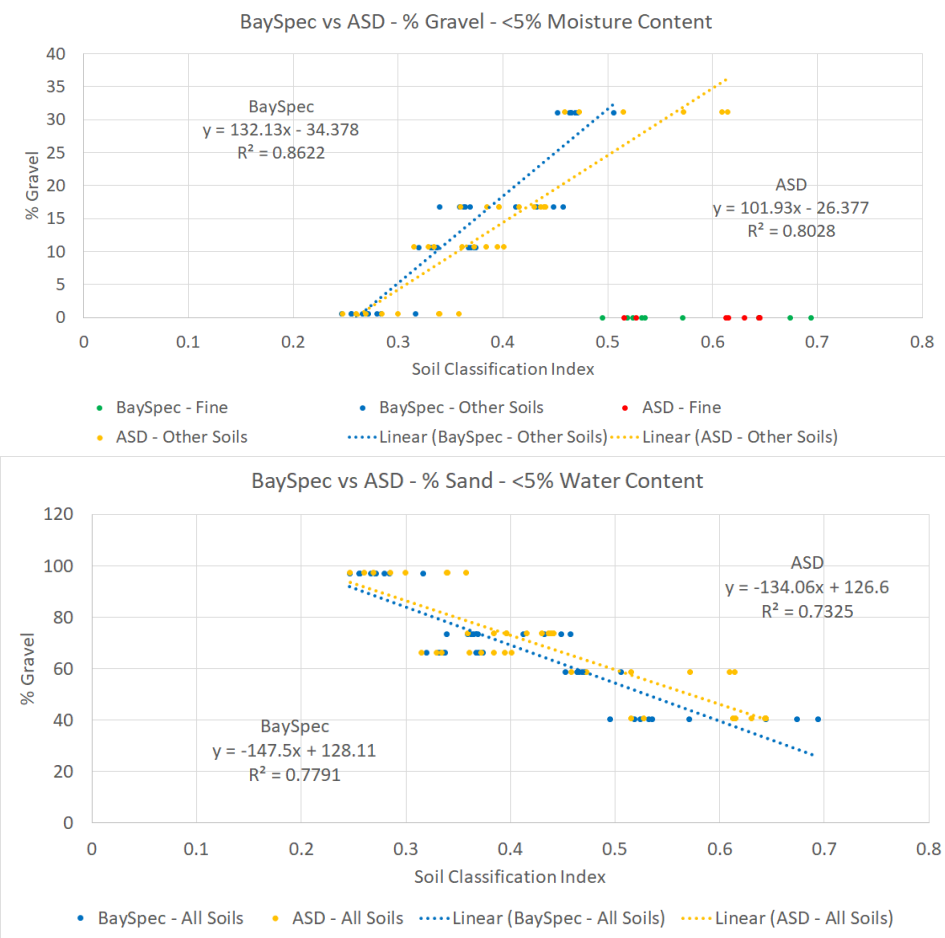

Figure 12: BaySpec and ASD plots for % Gravel vs. soil classification index (Top) and % Sand vs. soil classification index (Bottom)

Analysis and Discussion

Trends for both % gravel and % sand verses the soil classification index have been shown in figures 9 – 12. Both the BaySpec and ASD spectral radiometer detected these trends with R^2 values of 0.86 and 0.80 for % gravel and 0.78 and 0.73 for % sand. Figure 8 shows that various amount of water being added 0 – 4000 mL to the soil bins had little effect on the soil classification index. If the water content of the soil is known, then figure 10 allows for better prediction accuracy in all but the 3 - <5% water content for sand, and 0-<3% and 5 - <10% water content for gravel. In other cases the better prediction model comes from the 2% - <15% water content model in figure 9.

The reason for fine soil not working for the soil classification index estimating % gravel in both devices, may be due to the gravel content being zero, rather than having at least some gravel present as with the other four soils. Once the values of % gravel and % sand are known, the remaining makeup of the soil will consist of fine particles. Thus, giving one the entire particle size composition of the soil under examination. Specifics for the five soils tested are listed in Table 2. All the testing was done using pure soil samples and no organics present, which could skew the results when tested in the field.

As for figure 8 with the soil classification index remaining constant throughout adding varying milliliters of water to the soil, we assumed that 5 – 10 minutes was long enough for the water to soak into the soil. This may have led to skewing the moisture content: high water content in the top layer and drier in lower depths of the soils. The moisture content probes however do average over the entire soil depth, and the water had clearly soaked in beneath the visible surface of the soil.

Conclusions and future work:

In conclusion, the present approach for soil gradation using sieve analysis of in situ soil samples can be costly, or difficult to obtain. We have shown that using both a high resolution and a more cost-efficient hyperspectral camera, one can pick up intrinsic details about each of the five different soils used in this study.

With the improvement of cameras and cost to develop hyperspectral cameras reducing, these devices are going to become a much more readily available tool. These improvements in sensors have allowed us to create a soil classification index using values from the visible region of the reflectance spectrum. Utilizing the soil classification index, it is possible to remotely characterize the percent gravel, sand, and the remaining being fine soil. This method only requires the reflectance values at 550, 600, and 650 nm within a hyperspectral image. This soil classification index represents approximately the top 4-6 inches of the soil and remained fairly constant for each soil with increasing the moisture content. Knowing the approximate or actual moisture content of the soil helps improve the accuracy of the model. These details help to characterize and distinguish the soils within the Unified Soil Classification System (USCS) all by remotely collected hyperspectral data within the visible spectrum.

Keeping in mind the limitations, being that of different camera resolutions and what bands the hyperspectral cameras can pick up may not be exactly 550, 600, and 650 nm wavelengths. Different platforms and presence of organics in the soil may also have different results than that which this study has found.

In future work, we hope to expand this method into testing many different soil types outside the five used in this study. We also hope to look into variations of the predictions of percent gravel and sand, based on organics being present in the field. Finally, we also would like to take this study to UAV and satellite platforms and see how this study holds up at differing spectral and spatial resolutions.

Acknowledgements

We would like to thank the University of Michigan's Automotive Research Center (ARC), the U.S. Army Combat Capabilities Development Command Ground Vehicle Systems Center (CCDC - GVSC, formerly TARDEC), and Michigan Technological University (MTU) for funding this research. We would also like to thank the Keweenaw Research Center (KRC) for providing the logistics for data collection.

References

1. ASD Inc. (2010). ASD FieldSpec 3 - User Manual. Boulder, CO 80301.
2. ASTM International. (2017). D2487-17 Standard Practice for Classification of Soils for Engineering Purposes (Unified Soil Classification System). Retrieved from https://doi.org/10.1520/D2487-17
3. BaySpec, Inc. (2018). San Jose, CA 95131.
4. Campbell Scientific, Inc. (2018). CR1000X - Measurement and Control Datalogger.
5. Campbell Scientific, Inc. (1996). CS615 - Water Content Reflectometer. Logan, Utah 84321.
6. Cola, S., & Simonini, P. (2002). Mechanical behavior of silty soils of the Venice lagoon as a function of their grading characteristics. Canadian Geotechnical Journal, 39(4), 879–893. doi: 10.1139/t02-037
7. Dasch, J. and, Jayakumar P. (Eds). (2016) Final Report ET-148 Next-Generation NATO Reference Mobility Model (NRMM), NATO-AVT, 2016.
8. Demattê, J. A. M., Fiorio, P. R., & Araújo, S. R. (2010). Variation of Routine Soil Analysis When Compared with Hyperspectral Narrow Band Sensing Method. *Remote Sensing*, *2*(8), 1998–2016. doi: 10.3390/rs2081998
9. Fischer, C., & Kakoulli, I. (2006). Multispectral and hyperspectral imaging technologies in conservation: Current research and potential applications. Studies in Conservation,51(Sup1), 3-16. doi:10.1179/sic.2006.51.supplement-1.3
10. Kuenza, K., Towhata, I., Orense, R. P., & Wassan, T. H. (2004). Undrained torsional shear tests on gravelly soils. Landslides,1(3), 185-194. doi:10.1007/s10346-004-0023-3
11. Lucas, Y., & Gaggelli, J. (2002). Hyperspectral Detection of Sand. Retrieved from http://www.legos.obs-mip.fr/members/ouillon/publications/Ouillon_et_al_Proc2002.pdf?lang=en
12. Melgani, F., & Bruzzone, L. (2004). 13. Classification of Hyperspectral Remote Sensing Images with Support Vector Machines. *IEEE Transactions on Geoscience and Remote Sensing*, *42*(8), 1778–1790. Retrieved from https://ieeexplore.ieee.org/document/1323134
13. Minasny, B., & Mcbratney, A. (2016). Digital soil mapping: A brief history and some lessons. *Geoderma*, *264*, 301–311. doi: 10.1016/j.geoderma.2015.07.017
14. Selige, T., Böhner, J., & Schmidhalter, U. (2006). High resolution topsoil mapping using hyperspectral image and field data in multivariate regression modeling procedures. *Geoderma*, *136*(1-2), 235–244. doi: 10.1016/j.geoderma.2006.03.050
15. Shaw, G. A., & Burke, H.-hua K. (2003). Spectral Imaging for Remote Sensing. *Lincoln Laboratory Journal* , *14*(1). Retrieved from https://pdfs.semanticscholar.org/5ce6/339aca93ca69c00f4558c5a1bd08708d02e8.pdf
16. Simoni, A., & Houlsby, G. T. (2006). The Direct Shear Strength and Dilatancy of Sand–gravel Mixtures. *Geotechnical and Geological Engineering*, *24*(3), 523–549. doi: 10.1007/s10706-004-5832-6
17. Sousa, D., & Small, C. (2018). Multisensor Analysis of Spectral Dimensionality and Soil Diversity in the Great Central Valley of California. *Sensors*, *18*(2), 583. doi: 10.3390/s18020583

18. Stark, N., Mcninch, J., Wadman, H., Graber, H. C., Albatal, A., & Mallas, P. A. (2017). Friction angles at sandy beaches from remote imagery. *Géotechnique Letters*, *7*(4), 292–297. doi: 10.1680/jgele.17.00053
19. Vohland, M., Ludwig, M., Thiele-Bruhn, S., & Ludwig, B. (2017). Quantification of Soil Properties with Hyperspectral Data: Selecting Spectral Variables with Different Methods to Improve Accuracies and Analyze Prediction Mechanisms. *Remote Sensing*, *9*(11), 1103. doi: 10.3390/rs9111103
20. Zwissler, Bonnie, "Dust Susceptibility at Mine Tailings Impoundments: Thermal Remote Sensing for Dust Susceptibility Characterization and Biological Soil Crusts for Dust Susceptibility Reduction", Open Access Dissertation, Michigan Technological University, 2016.